Journal of Molecular Spectroscopy 337 (2017) 137–144

Contents lists available at ScienceDirect

Journal of Molecular Spectroscopy

journal homepage: www.elsevier.com/locate/jms

Influence of the position of the methoxy group on the stabilities of the *syn* and *anti* conformers of 4-, 5-, and 6-methoxyindole

Martin Wilke [a], Christian Brand [a,b], Josefin Wilke [a], Michael Schmitt [a,*]

[a] Heinrich-Heine-Universität, Institut für Physikalische Chemie I, D-40225 Düsseldorf, Germany
[b] University of Vienna, Faculty of Physics, VCQ, Boltzmanngasse 5, A-1090 Vienna, Austria

ARTICLE INFO

Article history:
Received 10 February 2017
In revised form 14 March 2017
Accepted 14 April 2017
Available online 20 April 2017

Dedicated to Walther Caminati.

Keywords:
Electronic spectroscopy
Structural analysis
Ab initio calculations
Conformational preferences
Methoxyindoles

ABSTRACT

Even though the two possible rotamers of methoxy-substituted indoles only differ in the orientation of a methoxy group, this slight geometry change can have a strong influence on the stabilities and further molecular properties of the conformers. In the present study, we evaluate the effect of the methyl group position on the presence of different conformers in molecular beam studies for the systems 4-, 5-, and 6-methoxyindole. By using rotationally resolved electronic Stark spectroscopy in combination with high level *ab initio* calculations the structures of the observable conformers have been assigned and reasons for the absence of the missing conformers discussed. Thereby, we could show that the relative ground state energies and isomerization barriers for both conformers strongly depend on the position of the methoxy group and are the main explanation for the absence of the *syn* conformers of 4-, and 5-methoxyindole.

1. Introduction

The basic concept that structure always precedes function has stimulated competing theories on molecular recognition like the older lock and key principle by Fischer [1], the more recent concept of induced fit by Koshland [2], and the conformational selection theory [3]. Today it seems confirmed that in many cases conformational selection is followed by conformational adjustment [4]. This means that allosteric binding at the receptor site of a protein induces a conformational change at another site. Thus, barriers to large amplitude motions have to be affected through the ligand molecule.

However, the term *structure* should include not only geometric effects on the interaction, but also electronic effects. Additionally, the magnitude and especially the direction of the permanent dipole moments in the electronic ground state strongly influence ligand-receptor interactions. In an intuitive picture the individual dipole moments of the polar groups in a molecule are summed vectorially, resulting in the overall dipole moment. However, Pratt and coworkers have shown that inductive effects may lead to breakdown of this rule [5]. Even for the electronic ground state theoretical predictions of electric dipole orientations can deviate considerably from the experimental one [6,7]. Also electronic excitations have been shown to dramatically change molecular dipole moments, in some cases a complete reorientation was observed [8].

For flexible molecules the dipole moment often depends on the specific conformation, stressing the influence of the conformational space. For methoxyindoles the problem of different rotamers in molecular beam experiments cannot be answered uniformly. In general, they can exist in two rotameric forms which are due to the twofold internal rotation of the methoxy group about the CO bond. For 6-methoxyindole (6MOI) two electronic origins bands at 33,722 and 33,952 cm^{-1} were observed in resonant enhanced multiphoton ionization (REMPI) spectra [9]. Our group could show that the shorter wavelength band at 33,716.58 cm^{-1} belongs to the *anti* rotamer, the other band at 33,948.12 cm^{-1} to the *syn* rotamer [10]. However, the excitation spectrum of 5-methoxyindole (5MOI) shows just a single origin band which could be shown to be due to the *anti* conformer [11–13]. Also the laser induced fluorescence spectrum of 4-methoxyindole (4MOI) consists of a single origin band at 35,309 cm^{-1} [12]. Hence, the question arises why the number of observed conformers in molecular beam experiments depends on the position of the substituent.

Here, we will study the position-dependent stability of the *syn* and *anti* conformers of 4-, 5-, and 6-methoxyindole. The structures of all molecules are shown in Fig. 1. Recently, the ground and excited state structures of 5MOI and 6MOI [13,10] and the dipole moments of 5MOI [6] have been presented. In the current

* Corresponding author.
E-mail address: mschmitt@uni-duesseldorf.de (M. Schmitt).

http://dx.doi.org/10.1016/j.jms.2017.04.009
0022-2852/

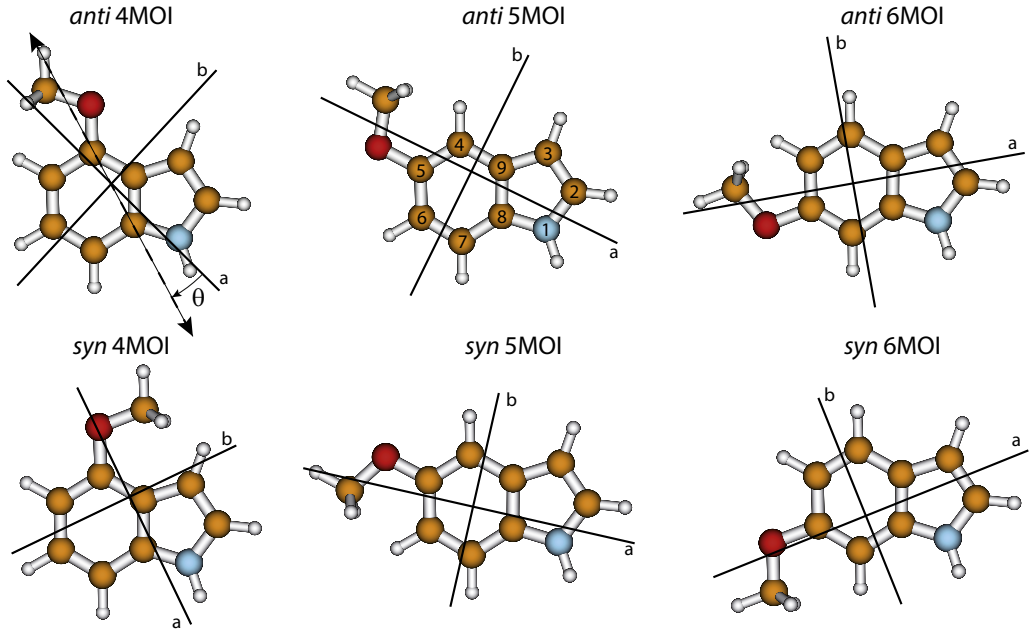

Fig. 1. Atomic numbering of the heavy atoms of indole and overview of the structures of both conformers of 4-, 5-, and 6-methoxyindole in their respective principal axis frame. For *anti* 4MOI a clockwise rotation of the TDM vector with respect to the *a*-axis is shown. The respective angle θ is defined to be negative.

contribution, we will extend the investigation to 4MOI, present the dipole moments of 4MOI and 6MOI and compare the whole class of methoxyindoles.

2. Experimental section

2.1. Experimental methods

4-Methoxyindole ($\geqslant 99\%$) and 6-Methoxyindole ($\geqslant 98\%$) were purchased from Sigma–Aldrich and Apollo Scientific. All samples were used without further purification. The experimental set-up for the rotationally resolved laser induced fluorescence spectroscopy is described in detail elsewhere [14,15]. In brief, the laser system consists of a single frequency ring dye laser (Sirah Matisse DS) operated with Rhodamine 110 and Rhodamine 6G pumped with 7.5 W of the 514 nm line of an Ar^+-ion laser (Coherent, Sabre 15 DBW). The dye laser output was coupled into an external folded ring cavity (Spectra Physics Wavetrain) for second harmonic generation. The resulting output power was constant at about 12 mW for 4-methoxyindole and 6-methoxyindole during the experiment. The molecular beam was formed by co-expanding 4-methoxyindole (6-methoxyindole), heated to 200 °C, and 300 mbar (700 mbar) of argon through a 200 µm nozzle into the vacuum chamber. The molecular beam machine consists of three differentially pumped vacuum chambers that are linearly connected by skimmers (1 mm and 3 mm, respectively) in order to reduce the Doppler width. The resulting resolution is 18 MHz (FWHM) in this set-up. In the third chamber, 360 mm downstream of the nozzle, the molecular beam crosses the laser beam at a right angle. The detection volume for the fluorescence light is formed by a concave mirror ($f = 25$ mm) in a distance of 50 mm below the crossing of molecular beam and laser beam and a plano-convex lens ($f = 50$ mm) at a distance of 50 mm above the molecular beam. The light is then focused onto the photocathode of a UV enhanced photomultiplier tube (Thorn EMI 9863QB) using a lens of $f = 130$ mm in a distance of 70 mm. For Stark measurements a parallel pair of electroformed nickel wire grids (18 mesh per mm, 50 mm diameter) with a transmission of 95% in the UV is used [6]. The grids have an effective distance is 23.49 ± 0.05 mm and are symmetrically aligned with respect to the laser beam. In the present experiment we used a field strength of 397.19 V/cm and a polarization of the laser which is parallel to the electric field. Due to technical reasons we always observe a weak contribution (20%) of light perpendicular polarized which is accounted for in the analysis.

2.2. Quantum chemical calculations

The equilibrium geometries of the electronic ground and the lowest excited singlet states were optimized using second-order approximate coupled-cluster (CC2) calculations employing the resolution-of-the-identity approximation (RI) [16–18], with Dunning's correlation consistent polarized valence triple zeta (cc-pVTZ) from the TURBOMOLE library [19,20]. Vibrational frequencies and zero-point corrections to the adiabatic excitation energies were obtained from numerical second derivatives using the NumForce script [21] implemented in the TURBOMOLE program suite [22]. A natural-bond-orbital (NBO) analysis [23] was performed at the optimzed geometries by using the wavefunctions from the CC2 calculations as implemented in the TURBOMOLE package [22].

2.3. Fits of the rovibronic spectra using evolutionary algorithms

The rotationally resolved electronic spectra are fit using evolutionary strategies (ES), described in detail in Refs. [24–27]. For the fits of the spectra we used the CMA-ES algorithm [28,29]. In this variant of global optimizers mutations are adapted via a covariance matrix adaptation (CMA) mechanism to find the global minimum even on rugged search landscapes that are additionally complicated due to noise, local minima and/or sharp bends.

The intensities of the rotational lines in the Stark spectra are calculated from the eigenvectors of the Stark Hamiltonian and the direction cosine matrix elements. The static electric field mixes the rovibronic eigenstates, so that J, K_a, and K_c are no good (pseudo-) quantum numbers any more, M is the only remaining good quantum number.

3. Results

3.1. Computational results

The relative energies of the *syn* and *anti* conformers of 4MOI, 5MOI, and 6MOI in the electronic ground and lowest electronically excited state are compiled in Fig. 2. In the electronic ground state the *anti* conformer is the most stable conformation for both 4- and 5-methoxyindole. The respective *syn* conformers lie 1160 cm^{-1} (4MOI) and 409 cm^{-1} (5MOI) higher in energy, including zero-point vibrational energy. For 6MOI the relative stability of the conformers is interchanged and the *syn* conformer is lowest in energy in the S_0. These rotamers can be interconverted via a rotation around the CO bond. The respective barriers for isomerization depend strongly on the position of the methoxy group at the indole chromophore. For 4MOI the barrier for *syn* → *anti* isomerization amounts only to 155 cm^{-1}, increases to 678 cm^{-1} for 5MOI and reaches 1134 cm^{-1} for 6MOI.

In the ground state all *anti* conformers lie within an energy band of ≈600 cm^{-1}. The same is true for the *syn* conformers. Excitation to the lowest excited singlet state leads to a pronounced shift in the relative energies of the molecular structures. For the *anti* conformer of 4MOI we observe a blue-shift of more than 2500 cm^{-1} compared to *anti* 5MOI. Also the relative stability of the conformers differ in the two electronic states. For 5MOI and 6MOI the energetic order of *syn* and *anti* is exchanged in the S_1 compared to the S_0. For 4MOI the *syn* and *anti* conformation become isoenergetic in the S_1. Here the strongest influence of the electronic excitation on the relative stability of the conformers is observed ($\Delta E \approx 1100$ cm^{-1}). This shows that the energetic ordering of the conformers strongly depends on the position of the substituent at the chromophore.

Table 1 summarizes the natural charges in the electronic ground and lowest electronically excited state of the methoxyindoles compared the one of indole itself, derived from an NBO analysis. The methoxy group donates electron density to the conjugated π-system via the mesomeric effect ($+M$). Calculating the electron density difference between the atoms of the methoxyindoles and indole in the ground state ($q_i^{MOI} - q_i^{indole}$) reveals that the electron density is primarily increased at the atoms in *ortho* and *para* position with respect to the methoxy group. Furthermore, the largest increase is observed at the *ortho* carbon atom to which the methyl group points, similar to the observation for 5-hydroxyindole [30]. Another remarkable point is that the addition of the methoxy group does not influence the electron distribution inside the pyrrole ring.

3.2. Experimental results

The rotationally resolved spectrum of the electronic origin of 4MOI is shown in Fig. 3. The molecular parameters extracted from the best CMA-ES fit of this spectrum are compiled in Table 2 and compared to the *ab initio* values for the two conformers of 4MOI. The assignment of the molecular structure is based on the rotational constants in the ground (A'', B'', C'') and excited state (A', B', C'). We observe excellent agreement between the experimental data and the predictions for the *anti* conformer. The angle

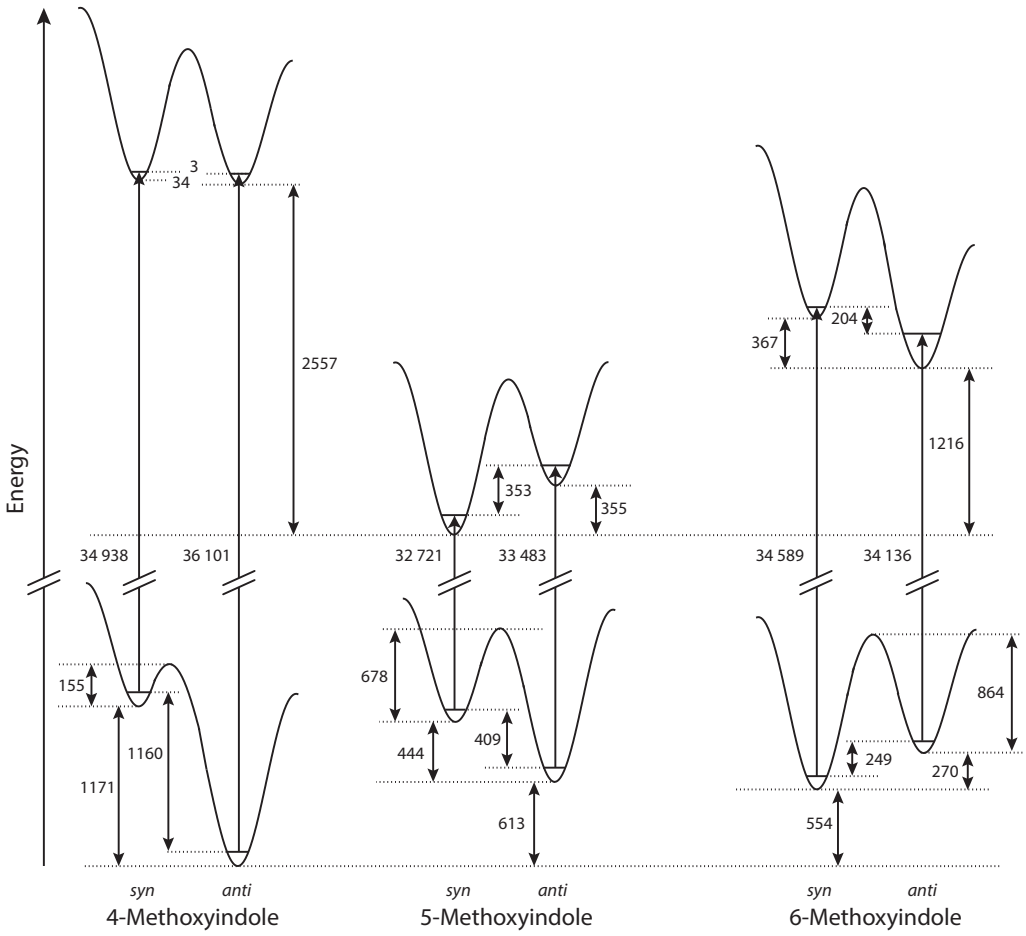

Fig. 2. Relative energies of both conformers of 4-, 5-, and 6-methoxyindole according to CC2/cc-pVTZ calculations. All energies are given in wavenumber [cm^{-1}].

Table 1
Natural charges from a natural population analysis (NPA) for both conformers of 4-, 5-, and 6-methoxyindole using the CC2/cc-pVTZ wave functions. For atomic labeling see Fig. 1.

	Indole	4-methoxyindole		5-methoxyindole		6-methoxyindole	
		Anti	*Syn*	*Anti*	*Syn*	*Anti*	*Syn*
				Ground state			
N1	−0.50	−0.50	−0.50	−0.50	−0.50	−0.51	−0.50
C2	−0.02	−0.03	−0.03	−0.02	−0.02	−0.03	−0.03
C3	−0.29	−0.28	−0.30	−0.29	−0.29	−0.29	−0.28
C4	−0.18	+0.32	+0.31	**−0.29**	**−0.24**	−0.17	−0.17
C5	−0.22	**−0.33**	**−0.27**	+0.28	+0.28	**−0.31**	**−0.25**
C6	−0.20	−0.18	−0.19	**−0.24**	**−0.29**	+0.30	+0.30
C7	−0.23	−0.26	−0.26	−0.21	−0.21	**−0.28**	**−0.34**
C8	+0.13	+0.14	+0.15	+0.11	+0.11	+0.15	+0.15
C9	−0.09	**−0.13**	**−0.16**	−0.07	−0.07	−0.11	−0.11
O1	–	−0.47	−0.48	−0.48	−0.48	−0.48	−0.47
C10	–	−0.21	−0.20	−0.21	−0.20	−0.20	−0.21
				Lowest electronically excited state			
N1	−0.45	−0.46	−0.47	−0.47	−0.45	−0.47	−0.50
C2	−0.09	−0.09	−0.10	−0.09	−0.10	+0.00	+0.02
C3	−0.24	−0.22	−0.26	−0.26	−0.25	−0.22	−0.25
C4	−0.23	+0.30	+0.29	**−0.32**	**−0.28**	−0.29	−0.29
C5	−0.12	**−0.21**	**−0.16**	+0.33	+0.33	**−0.35**	**−0.30**
C6	−0.25	−0.29	−0.30	**−0.31**	**−0.35**	+0.34	+0.34
C7	−0.29	−0.24	−0.23	−0.30	−0.29	**−0.38**	**−0.42**
C8	+0.14	+0.11	+0.13	+0.16	+0.15	+0.13	+0.15
C9	−0.07	**−0.18**	**−0.20**	−0.08	−0.09	−0.11	−0.07
O1	–	−0.43	−0.42	−0.40	−0.40	−0.41	−0.41
C10	–	−0.21	−0.21	−0.21	−0.21	−0.21	−0.21

Bold numbers show the largest differences of the natural charges between the *syn* and the *anti* rotamers.

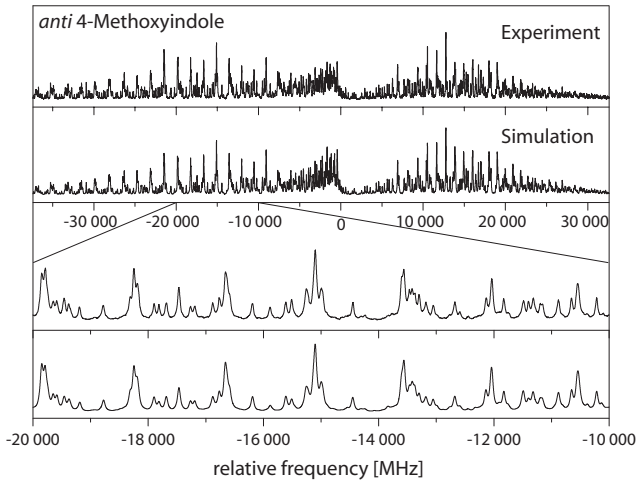

Fig. 3. Rotationally resolved spectrum of the electronic origin of the *anti* conformer of 4-methoxyindole, along with a simulation using the best CMA-ES fit parameters, given in Table 2.

θ, which defines the orientation of the transition dipole moment (TDM) with respect to the inertial *a*-axis, is predicted to be virtually identical for the two conformers within the accuracy of the calculations. A negative sign is defined by a clockwise rotation from the inertial *a*-axis onto the TDM vector, cf. Fig. 1. The experimentally observed value is in general agreement with the calculated ones. As the analysis of the band type yields only the projection of θ onto the inertial axes, we also measured a deuterated species of 4MOI to lift this ambiguity. The exchange of one atom by a heavier isotope rotates the *a*-axis towards this atom without affecting the orientation of the TDM [31,32]. Stirring 4MOI with deuterated methanol for a few hours leads to a new band in the fluorescence spectrum, which is blue-shifted by around 6 cm^{-1} to the undeuterated origin. The respective rotationally resolved spectrum of the electronic origin of the deuterated isotopomer can be found in Supporting Online Material. From the analysis of the rotational constants we can assign this spectrum to a species deuterated at the C_3-atom, cf. Fig. 1. The comparison of the computed rotational constants for all possible singly deuterated isotopomers from the *ab initio* structures with the experimental values is also given in Supporting Online Material. The increase in θ by 0.7°shows that the *a*-axis is rotated away from the TDM vector. Hence, we can determine the sign of θ to be negative. As it can be seen from Fig. 1, a value of −17.2° for θ corresponds to a TDM vector going almost through the pyrrolic nitrogen, which is typically attributed to the ^1L_a state in indole [33]. Following the nomenclature of Platt [34], the lowest two electronically excited states can be labeled as ^1L_a and ^1L_b. The transition to the former is dominated by a LUMO ← HOMO excitation and the latter can be described by a mixture of (LUMO + 1) ← HOMO and LUMO ← (HOMO − 1) contributions [35,13]. While the TDM vector orientation for 5MOI is ^1L_b like and almost orthogonal to the ^1L_a vector [13], the change of the methoxy group to position 4 or 6 introduces LUMO ← HOMO contributions in the S_1 state. This leads to a reorientation of the TDM vector [36,37].

The magnitude of the inertial defect ΔI, which is a measure of the non-planarity of a molecule, points towards a mainly planar structure of 4MOI in both states. The slightly negative value stems from the two hydrogen atoms of the methyl group which are not within the aromatic plane.

Additionally, we recorded rotationally resolved electronic Stark spectra at our maximum field strength of 397.19 V/cm to determine the ground and excited state dipole moments of 4MOI and 6MOI. However, for *anti* 6MOI the effect of the applied field strength is not sufficient to result in a detectable change in the spectrum. The respective values for 5MOI have been published previously [7]. During the analysis of the spectrum all molecular parameter except for the dipole moment and its orientation were kept constant at the values from the fit of the field free spectrum (see Table 2 and Ref. [10]). Fig. 4 shows a small portion of the electronic origin of *syn* 6MOI compared to the Stark spectrum, along with the simulations of the CMA-ES fit. The Stark spectrum of *anti* 4MOI can be found in Supporting Online Material. The resulting

Table 2
Experimentally observed molecular parameters of 4-methoxyindole in the S_0 and S_1 state and the respective values at CC2/cc-pVTZ level of theory. The undeuterated spectrum is denoted with d_0, the deuterated with [d-C_3]. Changes of the rotational constants are defined as: $\Delta B_g = B'_g - B''_g$, with B_g as rotational constants with respect to the inertial axes $g = a,\ b,\ c$. Double-primed constants belong to the ground state and single-primed to the excited state. ν_0 is the energy of the electronic transition and τ the excited state lifetime. For more details see text.

	Experiment		Theory, d_0	
	d_0	[d-C_3]	*Anti*	*Syn*
A''/MHz	1971.9(2)	1917.91(19)	1981.9	1623.3
B''/MHz	1005.77(4)	1005.42(3)	1007.0	1227.7
C''/MHz	669.11(3)	662.67(2)	670.6	702.2
$\Delta I''$/amu Å^2	−3.46	−3.52	−3.20	−3.21
A'/MHz	1927.7(2)	1875.47(27)	1935.8	1580.8
B'/MHz	992.76(4)	992.34(3)	993.1	1223.3
C'/MHz	658.43(3)	652.09(2)	659.1	692.7
$\Delta I'$/amu Å^2	−3.67	−3.73	−3.21	−3.21
θ/°	±17.2(1)	±17.9(1)	−7	−3
ν_0/cm^{-1}	35302.24(1)	35308.20(1)	36,101	34,938

ground and excited state dipole moments μ, the individual components μ_i along the main inertial axes $i = a,\ b$(the value of μ_c is zero by symmetry) and the angle θ_D of the permanent dipole moment with the inertial *a*-axis are summarized in Table 3 and compared to the values of 5MOI. Since electronic Stark spectroscopy only yields the unsigned values of the Cartesian components, the orientation of the dipole moment vector and thus the sign of θ_D remains undetermined. This can be removed by comparison to the calculations.

In the ground state the experimental dipole moment of *anti* 4MOI is in very good agreement with the calculated one. Regarding the individual components, theory overestimates μ_a and underestimates μ_b only slightly. Hence, the magnitude of θ_D is well reproduced and the negative sign can be adapted from theory. In the electronically excited state the permanent dipole is reduced to 0.27 D. For such a small dipole moment the error of the calculations is on the same order as the value itself and we observe a large deviation in θ_D between theory and experiment. For 6MOI the overall magnitude of the dipole moment and its components in the S_0 are well described by theory as well. In the excited state both μ_a and μ_b are overestimated by 25% which results in an excellent agreement regarding the orientation of the dipole moment.

From Table 3 it becomes apparent that the dipole moment of the *anti* conformer is always smaller in magnitude than the one of the respective *syn* conformer, both in the ground and the electronically excited state. A general and intuitive model to estimate the magnitude and orientation of molecular dipole moments consists of the vector sum of the respective bond or fragment dipole moments. Neglecting inductive effects, this model works pretty well for the electronic ground state, while it must be treated quite carefully for the electronically excited states [5–7,38,39]. Here, we will concentrate on the ground state and apply the vector additivity model for the three investigated systems. Fig. 5 shows the vector addition ($\vec{\mu}_{MOI} = \vec{\mu}_{indole} + \vec{\mu}_{anisole}$) of the experimental ground state dipole moment vectors of indole [40] and anisole [41] in order to estimate the magnitude and orientation of the ground state dipole moments of the *anti* conformers of 4MOI and 6MOI as well as of the *syn* conformer of 6MOI. The resulting dipole moments of the methoxyindoles (0.81 D for *anti* 4MOI, 1.36 D for *anti* 5MOI and 2.98 D for *syn* 6MOI) are in good agreement with the experimental values from Table 3.

4. Discussion

The relative intensity of conformers in an electronic spectrum depends on a number of parameters. The population of the initial state has a major influence as it determines how many molecules

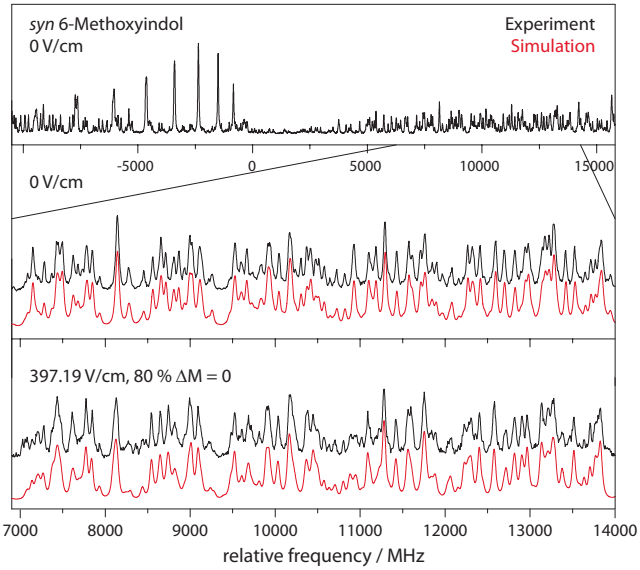

Fig. 4. Rovibronic spectrum of the electronic origin of the *syn* conformer of 6-methoxyindole at 0 V/cm with a zoomed part of the spectrum at 0 V/cm and 397.19 V/cm with both field configurations along with a simulation using the best CMA-ES fit parameters, given in Table 3.

can be excited. However, also other effects play a role like the conformer-dependent oscillator strength [42], Franck-Condon factors [43], quantum yields [44,45], or vibronic couplings [46,47]. In the following we will address these points for the discussed structures.

The most intuitive explanation for the presence or absence of different conformers in molecular beam studies comes from the comparison of the relative energies in the ground state. While for 4MOI and 5MOI only the *anti* conformer is observed experimentally [11–13], both conformers are present for 6MOI [9,10]. For 5MOI this was explained with a combined effect of the stabilization of the *anti* conformer compared to the respective *syn* counterpart and the low barrier separating both conformers [6]. Consequently, all of the population of the *syn* conformer gets converted into the *anti* structure via collisions with the seed gas in the adiabatic expansion. This applies even more to 4MOI, where the energy gap between both conformers is larger and the barrier smaller for *syn* → *anti*-isomerization. These explanations are in agreement with calculations made by Oliver et al., who determined an abundance of 75% for *anti* 5MOI and 99% *anti* 4MOI in the molecular beam at a temperature of 400 K before the expansion

Table 3
Summary of the calculated and experimental permanent electric dipole moments μ and their components μ_i along the main inertial axes $i = a,\ b$ of both conformers of 4-, 5- and 6-methoxyindole. Double primed parameters belong to the electronic ground and single primed to the excited state. Additionally the angle θ_D of the dipole moment vector with the main inertial a-axis is given. A positive sign of this angle means a clockwise rotation of the dipole moment vector onto the a-axis in the principal axis frame of the molecules shown in Fig. 1. The uncertainties of the parameters are given in parentheses and are obtained as standard deviations by performing a quantum number assigned fit.

	4-Methoxyindole			5-Methoxyindole [6]			6-Methoxyindole		
	Experiment	Theory		Experiment	Theory		Experiment	Theory	
	Anti	*Anti*	*Syn*	*Anti*	*Anti*	*Syn*	*Syn*	*Anti*	*Syn*
μ''_a/D	0.82(9)	0.93	2.06	1.53(1)	1.64	1.00	0.22(20)	0.25	0.29
μ''_b/D	0.56(8)	0.43	1.93	0.42(6)	0.07	2.35	2.88(1)	0.79	3.01
μ''/D	0.99(12)	1.03	2.82	1.59(3)	1.64	2.56	2.89(3)	0.83 [10]	3.08 [10]
θ''_D/°	±34(4)	−25	+43	±15(1)	+2	−67	±86(1)	−72 [10]	−85 [10]
μ'_a/D	0.00	0.11	0.77	0.41(11)	0.29	0.49	0.42(11)	0.66	0.54
μ'_b/D	0.27(17)	0.15	1.93	1.06(2)	1.05	1.70	3.43(1)	1.75	4.28
μ'/D	0.27(17)	0.19	2.08	1.14(6)	1.09	1.77	3.46(2)	1.87 [10]	4.31 [10]
θ'_D/°	90.0	−54	+69	±69(1)	−75	−106	± 83(1)	−69 [10]	−83 [10]

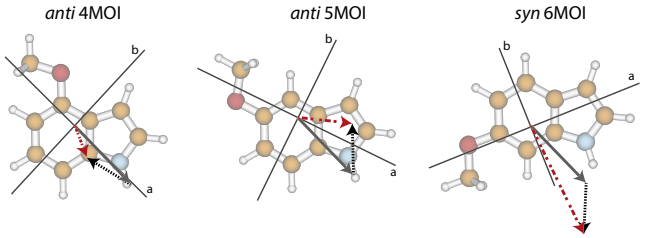

Fig. 5. Vector addition of the experimental ground state dipole moment of indole (grey solid line) and the dipole moment of anisole (black dashed line). The resulting vector (red dash-dotted line) represents the estimated ground state dipole moment of the respective methoxyindole. For the sake of clarity and a better comparison to the values in Table 3, they are shifted to the center of mass. (For interpretation of the references to color in this figure legend, the reader is referred to the web version of this article.)

Table 4
Summary of the fluorescence quantum yields Q_f of the experimentally observed conformers of the investigated methoxyindoles. For more details see text.

	Anti 4MOI	*Anti* 5MOI	*Anti* 6MOI	*Syn* 6MOI
f	0.09	0.08 [6]	0.13 [10]	0.10 [10]
ν_{fi}/cm^{-1}	36 204	33 271	33 598	34 353
τ_{exp}/ns	3.0(1)	6.7 [13]	4.3(1) [10]	4.5(1) [10]
Q_f	0.3	0.4	0.4	0.4

[48]. For 6MOI the barrier is sufficiently high between the two conformers that no conversion takes place and both conformers can be investigated.

Recently, we could show that large geometry changes upon excitation, and thus the decreasing Franck-Condon factors for the origin excitations, can also play a major role in the discussion

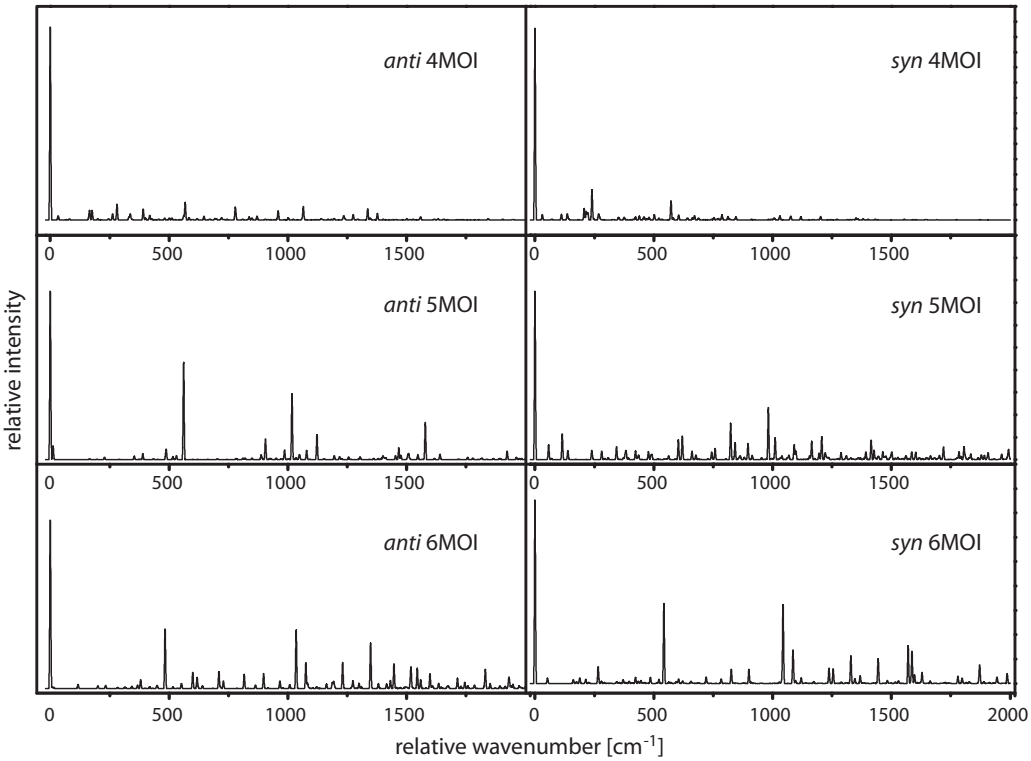

Fig. 6. Franck-Condon simulations of the excitation spectra of the *syn* and *anti* conformers of 4-, 5-, and 6-methoxyindole at CC2/cc-pVTZ level of theory.

about the presence of different conformers [43]. In order to examine this effect, Frank-Condon simulations of the excitation spectra have been made for all investigated systems and are compiled in Fig. 6. They have been obtained from the *ab initio* optimized ground and excited state structures of each conformer and the respective Hessian using the program FCFit [49,50]. It computes the excitation spectrum in the FC approximation in the basis of multidimensional harmonic oscillator wavefunctions.

The 0,0 transition is the strongest transition, independent of the position and conformation of the methoxy group. While for 4MOI almost none of the oscillator strength is distributed over higher vibronic levels, there are several vibronic levels of 5MOI and 6MOI with increased intensities. However, the Franck-Condon simulations for the *syn* conformers do not show significant changes compared to the respective *anti* counterparts. Consequently, the Franck-Condon factors cannot be used to explain the absence of the *syn* conformers of 4MOI and 4MOI.

Conformer-dependent couplings to other states may also alter the relative intensity of transitions in the fluorescence spectrum. Although vibronic couplings to higher lying electronic states can be excluded as we observe the S_1 in its vibrationless ground state, conformer-dependent couplings to non-radiative decay channels may affect the relative intensities in the fluorescence spectrum. This can be tested by determining the fluorescence quantum yields Q_f of the experimentally observed conformers. It can be calculated from the ratio of the pure radiative life time τ_{nat}, which is defined as the inverse of the fluorescence rate constant k_f, and the experimental lifetime τ_{exp}, which includes all radiative and non-radiative deactivation paths. The latter one has been determined from a fit of the Lorentzian contribution to Voigt profiles.

$$Q_f = \frac{k_f}{k_f + \sum k_{nr}} = \frac{k_f}{\sum k_i} = \frac{\tau_{exp}}{\tau_{nat}} \tag{1}$$

The experimental lifetime depends on the calculated transition frequency ν_{fi} and transition dipole moment μ_{fi} given in Debye for the vertical emission from the lowest excited to the electronic ground state at the optimized S_1 state geometry.

$$\tau_{nat} = \frac{c^3}{8\pi^2 \nu_{fi}^3} \frac{3\epsilon_0 \hbar}{\mu_{fi}^2} \tag{2}$$

$$\mu_{fi} = \sqrt{\frac{f\hbar e^2}{4m_e \nu_{fi}}} \tag{3}$$

In Table 4 the oscillator strengths f and transition frequencies ν_{fi} obtained from the calculations as well as the experimentally determined life times τ_{exp} for all experimentally observed conformers are compiled, together with the resulting fluorescence quantum yields Q_f.

All these values are well within the spread of the other conformers and, hence, cannot be held responsible for the missing two rotamers as well.

5. Conclusion

Rotationally resolved electronic Stark spectra of *anti* 4MOI and *syn* 6MOI have been recorded and analyzed in order to determine the structures and dipole moments in the ground and lowest electronically excited state. The absence of the *syn* conformers for 4MOI and 5MOI in the spectra has been discussed in the context of relative population and emission properties. As the emission properties are rather homogeneous for 4MOI, 5MOI and 6MOI, we conclude that the relative population of the rotamers in the molecular beam is the reason for the experimental results. This implies that a difference of less than 200 cm^{-1} in the barrier height for isomerization decides whether both conformers are present in a molecular beam (6MOI) or only one of them (5MOI).

Acknowledgements

We gratefully acknowledge the help of Leo Meerts for making available the analysis of the electronic Stark spectrum with the CMA-ES algorithm. Michael Schmitt thanks the Deutsche Forschungsgemeinschaft (SCHM 1043/12-3)) for financial support of this work. Computational support and infrastructure was provided by the "Center for Information and Media Technology" (ZIM) at the Heinrich-Heine-University Düsseldorf (Germany).

Appendix A. Supplementary material

Supplementary data associated with this article can be found, in the online version, at http://dx.doi.org/10.1016/j.jms.2017.04.009.

References

[1] E. Fischer, Einfluss der Configuration auf die Wirkung der Enzyme, Ber. Dtsch. Chem. Ges. 27 (1894) 2985–2993.
[2] D.E. Koshland, Application of a theory of enzyme specificity to protein synthesis, Proc. Natl. Acad. Sci. USA 44 (1958) 98–123.
[3] B. Ma, S. Kumar, C.-J. Tsai, R. Nussinov, Folding funnels and binding mechanisms, Protein Eng. Des. Select. 12 (1999) 713–720.
[4] P. Csermely, R. Palotai, R. Nussinov, Induced fit, conformational selection and independent dynamic segments: an extended view of binding events, Trends Biochem. Sci. 35 (2010) 539–546.
[5] D.R. Borst, T.M. Korter, D.W. Pratt, On the additivity of bond dipole moments. Stark effect studies of the rotationally resolved electronic spectra of aniline, benzonitrile and aminobenzonitrile, Chem. Phys. Lett. 350 (2001) 485–490.
[6] J. Wilke, M. Wilke, W.L. Meerts, M. Schmitt, Determination of ground and excited state dipole moments via electronic stark spectroscopy: 5-methoxyindole, J. Chem. Phys. 144 (4) (2016) 044201.
[7] J. Wilke, M. Wilke, C. Brand, W.L. Meerts, M. Schmitt, On the additivity of molecular fragment dipole moments of 5-substituted indole derivatives, ChemPhysChem 17 (2016) 2736–2743.
[8] J.A. Thomas, J.W. Young, A.J. Fleisher, L. Alvarez-Valtierra, D.W. Pratt, Stark-effect studies of 1-phenylpyrrole in the gas phase. dipole reversal upon electronic excitation, J. Chem. Phys. Lett. 1 (2010) 2017–2019.
[9] M. Sulkes, I. Borthwick, Enhanced photophysical effects in indole due to C-6 chemical group substitutions, Chem. Phys. Lett. 279 (1997) 315–318.
[10] C. Brand, O. Oeltermann, M. Wilke, M. Schmitt, Position matters: high resolution spectroscopy on 6-methoxyindole, J. Chem. Phys. 138 (2013) 024321.
[11] Y. Huang, M. Sulkes, Jet-cooled solvent complexes with indoles, J. Phys. Chem. 100 (1996) 16479.
[12] Y. Huang, M. Sulkes, Anomalously short fluorescence lifetimes in jet cooled 4-hydroxyindole. Evidence for excited state tautomerism and proton transfer in clusters, Chem. Phys. Lett. 254 (1996) 242–248.
[13] C. Brand, O. Oeltermann, D.W. Pratt, R. Weinkauf, W.L. Meerts, W. van der Zande, K. Kleinermanns, M. Schmitt, Rotationally resolved electronic spectroscopy of 5-methoxyindole, J. Chem. Phys. 133 (2010) 024303.
[14] M. Schmitt, Hochauflösende elektronische Spektroskopie an Molekülen und Clustern, Habilitation, Heinrich-Heine-Universität, Math. Nat. Fakultät, Düsseldorf, 2000.
[15] M. Schmitt, J. Küpper, D. Spangenberg, A. Westphal, Determination of the structures and barriers to hindered internal rotation of the phenol-methanol cluster in the S_0 and S_1 state, Chem. Phys. 254 (2000) 349–361.
[16] C. Hättig, F. Weigend, CC2 excitation energy calculations on large molecules using the resolution of the identity approximation, J. Chem. Phys. 113 (2000) 5154–5161.
[17] C. Hättig, A. Köhn, Transition moments and excited-state first-order properties in the coupled cluster model CC2 using the resolution-of-the-identity approximation, J. Chem. Phys. 117 (2002) 6939–6951.
[18] C. Hättig, Geometry optimizations with the coupled-cluster model CC2 using the resolution-of-the-identity approximation, J. Chem. Phys. 118 (2002) 7751–7761.
[19] R. Ahlrichs, M. Bär, M. Häser, H. Horn, C. Kölmel, Electronic structure calculations on workstation computers: the program system turbomole, Chem. Phys. Lett. 162 (1989) 165–169.
[20] T.H. Dunning Jr., Gaussian basis sets for use in correlated molecular calculations. I. The atoms boron through neon and hydrogen, J. Chem. Phys. 90 (1989) 1007–1023.
[21] P. Deglmann, F. Furche, R. Ahlrichs, An efficient implementation of second analytical derivatives for density functional methods, Chem. Phys. Lett. 362 (2002) 511–518.

[22] Turbomole v6.5 2013, A Development of University of Karlsruhe and Forschungszentrum Karlsruhe GmbH, 1989–2007, TURBOMOLE GmbH, Since 2007, 2013. <http://www.turbomole.com>.
[23] A.E. Reed, R.B. Weinstock, F. Weinhold, Natural population analysis, J. Chem. Phys. 83 (1985) 735–746.
[24] W.L. Meerts, M. Schmitt, G. Groenenboom, New applications of the genetic algorithm for the interpretation of high resolution spectra, Can. J. Chem. 82 (2004) 804–819.
[25] W.L. Meerts, M. Schmitt, A new automated assign and analyzing method for high resolution rotational resolved spectra using genetic algorithms, Phys. Scripta 73 (2005) C47–C52.
[26] W.L. Meerts, M. Schmitt, Application of genetic algorithms in automated assignments of high-resolution spectra, Int. Rev. Phys. Chem. 25 (2006) 353–406.
[27] M. Schmitt, W.L. Meerts, Rotationally resolved electronic spectroscopy and automatic assignment techniques using evolutionary algorithms, in: M. Quack, F. Merkt (Eds.), Handbook of High Resolution Spectroscopy, John Wiley and Sons, 2011.
[28] A. Ostermeier, A. Gawelczyk, N. Hansen, Step-Size Adaptation Based on Non-Local Use of Selection Information, Lecture Notes in Computer Science: Parallel Problem Solving from Nature (PPSN III), Springer, 1994.
[29] N. Hansen, A. Ostermeier, Completely derandomized self-adaptation in evolution strategies, Evol. Comput. 9 (2001) 159–195.
[30] O. Oeltermann, C. Brand, M. Wilke, M. Schmitt, Ground and electronically excited singlet state structures of the *syn* and *anti* rotamers of 5-hydroxyindole, J. Phys. Chem. A 116 (2012) 7873–7879.
[31] M. Schmitt, D. Krügler, M. Böhm, C. Ratzer, V. Bednarska, I. Kalkman, W.L. Meerts, A genetic algorithm based determination of the ground and excited ^1L_b state structure and the orientation of the transition dipole moment of benzimidazole, Phys. Chem. Chem. Phys. 8 (2006) 228–235.
[32] C. Kang, J.T. Yi, D.W. Pratt, High resolution electronic spectra of 7-azaindole and its Ar atom van der Waals complex, J. Chem. Phys. 123 (2005) 094306.
[33] C. Brand, J. Küpper, D.W. Pratt, W.L. Meerts, D. Krügler, J. Tatchen, M. Schmitt, Vibronic coupling in indole: I. Theoretical description of ^1L_a and ^1L_b interactions and the absorption spectrum, Phys. Chem. Chem. Phys. 12 (2010) 4968–4997.
[34] J.R. Platt, Classification of spectra of cata-condensed hydrocarbons, J. Chem. Phys. 17 (1949) 484–495.
[35] L. Serrano-Andrés, B.O. Roos, Theoretical study of the absorption and emission spectra of indole in the gas phase and in a solvent, J. Am. Chem. Soc. 118 (1996) 185–195.
[36] B. Albinsson, B. Nordén, Excited-state properties of the indole chromophore – electronic-transition moment directions from linear dichroism measurements – effect of methyl and methoxy substituents, J. Phys. Chem. 96 (1992) 6204.
[37] J. Wilke, M. Wilke, C. Brand, J.D. Spiegel, C.M. Marian, M. Schmitt, Modulation of the L_a/L_b mixing in an indole derivative: a position-dependent study using 4-, 5-, and 6-fluoroindole, J. Phys. Chem. A 121 (8) (2017) 1597–1606, http://dx.doi.org/10.1021/acs.jpca.6b12605.
[38] D.M. Miller, P.J. Morgan, D.W. Pratt, On the electric dipole moments of asymmetric tops: measurement by high-resolution electronic spectroscopy in the gas phase, J. Phys. Chem. A 113 (25) (2009) 6964–6970.
[39] J.A. Reese, T.V. Nguyen, T.M. Korter, D.W. Pratt, Charge redistribution on electronic excitation. Dipole moments of *cis*- and *trans*-3-aminophenol in their S_0 and S_1 electronic states, J. Am. Chem. Soc. 126 (2004) 11387–11392.
[40] C. Kang, T.M. Korter, D.W. Pratt, Experimental measurement of the induced dipole moment of an isolated molecule in its ground and electronically excited states: indole and indole-H_2O, J. Chem. Phys. 122 (2005) 174301.
[41] O. Desyatnyk, L. Pszczolkowski, S. Thorwirth, T.M. Krygowski, Z. Kisiel, The rotational spectra, electric dipole moments and molecular structures of anisole and benzaldehyde, Phys. Chem. Chem. Phys. 7 (2005) 1708–1715.
[42] C. Brand, W.L. Meerts, M. Schmitt, How and why do transition dipole moment orientations depend on conformer structure?, J Phys. Chem. A 115 (2011) 9612–9619.
[43] M. Wilke, M. Schneider, J. Wilke, J.A. Ruiz-Santoyo, J.J. Campos-Amador, M.E. González-Medina, L. Álvarez-Valtierra, M. Schmitt, Rotationally resolved electronic spectroscopy study of the conformational space of 3-methoxyphenol, J. Mol. Struct. doi:http://dx.doi.org/10.1016/j.molstruc.2016.10.096.
[44] B. Donzel, P. Gaudchon, P. Wahl, Conformation in the excited state of two tryptophanyl diketopiperazines, J. Am. Chem. Soc. 96 (3) (1974) 801–808.
[45] O.K. Gasymov, A.R. Abduragimov, B.J. Glasgow, Tryptophan rotamer distribution revealed for the α-helix in tear lipocalin by site-directed tryptophan fluorescence, J. Phys. Chem. B 116 (2012) 13381–13388.
[46] E.G. Buchanan, P.S. Walsh, D.F. Plusquellic, T.S. Zwier, Excitonic splitting and vibronic coupling in 1,2-diphenoxyethane: conformation-specific effects in the weak coupling limit, J. Chem. Phys. 138 (2013) 204313.
[47] C.P. Rodrigo, C.W. Müller, N.R. Pillsbury, W.H. James III, D.F. Plusquellic, T.S. Zwier, Conformer-specific vibronic spectroscopy and vibronic coupling in a flexible bichromophore: bis-(4-hydroxyphenyl)methane, J. Chem. Phys. 134 (2011) 164312.
[48] T.A.A. Oliver, G.A. King, M.N.R. Ashfold, Position matters: competing O-H and N-H photodissociation pathways in hydroxy- and methoxy-substituted indoles, Phys. Chem. Chem. Phys. 13 (2011) 14646–14662.
[49] D. Spangenberg, P. Imhof, K. Kleinermanns, The S_1 state geometry of phenol determined by simultaneous Franck-Condon and rotational constants fits, Phys. Chem. Chem. Phys. 5 (2003) 2505–2514.
[50] R. Brause, M. Schmitt, D. Spangenberg, K. Kleinermanns, Determination of the excited state structure of 7-azaindole using a Franck-Condon analysis, Mol. Phys. 102 (2004) 1615–1623.